Supplementary Information

Circularly polarized luminescence enlargement from crystals to oriented films of enantiopure 2D hybrid perovskite

Xuan-Hui Zhao,[a,b] Na-Na Li,[a,c] Jing Peng,[a] Jun Xu,[a] Peng Luo,[a] Xi-Yan Dong[a,b] and Xiaozong Hu[b*]*

*Correspondence: dongxiyan0720@hpu.edu.cn (X. Y. Dong), huxz@zzu.edu.cn (X. Hu)

Experimental section

Reagents and Materials Used. (R)-1-4-fluorophenethylamine (***R*-FMBA**, 98%) and (S)-1-(4-fluorophenethylamine (***S*-FMBA**, 98%) were purchased from Bidepharm Ltd. (Shanghai, China). The ***rac*-FMBA** is obtained by mixing ***R*-FMBA** and ***S*-FMBA** in equal amount Lead(II) bromide ($PbBr_2$, 99%) was purchased from Aladdin Ltd. (Shanghai, China). Hydrobromic acid (HBr), dichloromethane (DCM) were purchased from Kermel Ltd. (Tianjin, China).

Materials Preparation. Synthesis and purification of (*R*-FMBA)$_2$PbBr$_4$ (***R*-1**) and (*S*-FMBA)$_2$PbBr$_4$ (***S*-*1***). Lead (II) bromide (183.5 mg, 0.5 mmol) and ***R*-FMBA** (140 mg, 1 mmol) were mixed and dissolved in HBr (10 mL). The mixture was heated and stirred to form a transparent precursor solution, and after the volatilization of the solvent, ***R*-1** flake crystals were obtained. The obtained crystals were thoroughly washed with DCM and then dried in vacuo, and pure ***R*-1** ware was obtained. The method for obtaining ***S*-1** is similar to that of ***R*-1**. Synthesis and purification of and (*rac*-FMBA)$_8$Pb$_3$Br$_{14}$·2H$_2$O (***rac*-1**). ***R*-FMBA** (70 mg, 0.05 mmol) and ***S*-FMBA** (70 mg, 0.05 mmol) are mixed in equal amounts with $PbBr_2$ (183.5 mg, 0.5 mmol) and dissolved in HBr, heated and stirred until clear to obtain acicular crystal ***rac-1***. The purification process is the same as that of ***R*-1**.

Thin films Preparation. Dissolve 40 mg of ***R*-1** or ***S*-1**crystals in 100 μL of DMF, drop the solution onto the quartz plate on the spin coater (acetone ultrasonic for 15 min, ethanol ultrasonic for 15 min, dried and treated with plasma cleaning machine for 15 min). Turn on the spin coater for 1000 r/min for 10 s and 3000 r/min for the 20 s immediately. After annealing at 90 ℃ for 10 min, uniform ***R*-1** or ***S*-1** films were obtained. It is worth noting that films of different sizes perpendicular to the bottom can be obtained after annealing in the above operation.

Material Characterizations. Crystallographic data collection and refinement of the structure. Single-crystal X-ray diffraction measurements of ***R*-1**, ***S*-1** and ***rac*-1** were performed on a Rigaku XtaLAB Pro diffractometer. Data collection and reduction were

performed using the program CrysAlisPro.[1] All the structures were solved with direct methods (SHELXS)[2] and refined by full-matrix least-squares on F2 using OLEX2,[3] which utilizes the SHELXL-2015 module.[4] All the atoms were refined anisotropically. Hydrogen atoms were placed in calculated positions refined using idealized geometries and assigned fixed isotropic displacement parameters. The crystal structures are visualized by DIAMOND 3.2. Powder X-ray diffraction (PXRD) patterns of ***R*-1**, ***S*-1** and ***rac*-1** were collected at room temperature in the air using an X'Pert PRO diffractometer. Thermogravimetry analyses (TGA) were performed on a TA Q50 system under N_2 atmosphere (flow rate = 60 mL/min) in the temperature range 30 - 800 °C at a heating rate of 10 °C/min. UV-visible diffuse reflectance spectra of samples were recorded at room temperature in the range of 240 - 800 nm using a UH4150 spectrophotometer equipped with an integrating sphere. The room temperature steady-state spectroscopy, time-resolved photoluminescence (PL), temperature-dependent emission spectra and photoluminescence quantum yield were measured on the HORIBA FluoroLog-3 fluorescence spectrometer. The circular dichroism (CD) spectra of powder samples were measured on JASCO J-1500 by potassium bromide tablet pressing method. Circularly polarized luminescence (CPL) spectra of powder samples were measured on a JASCO CPL-300.

Supporting Figures

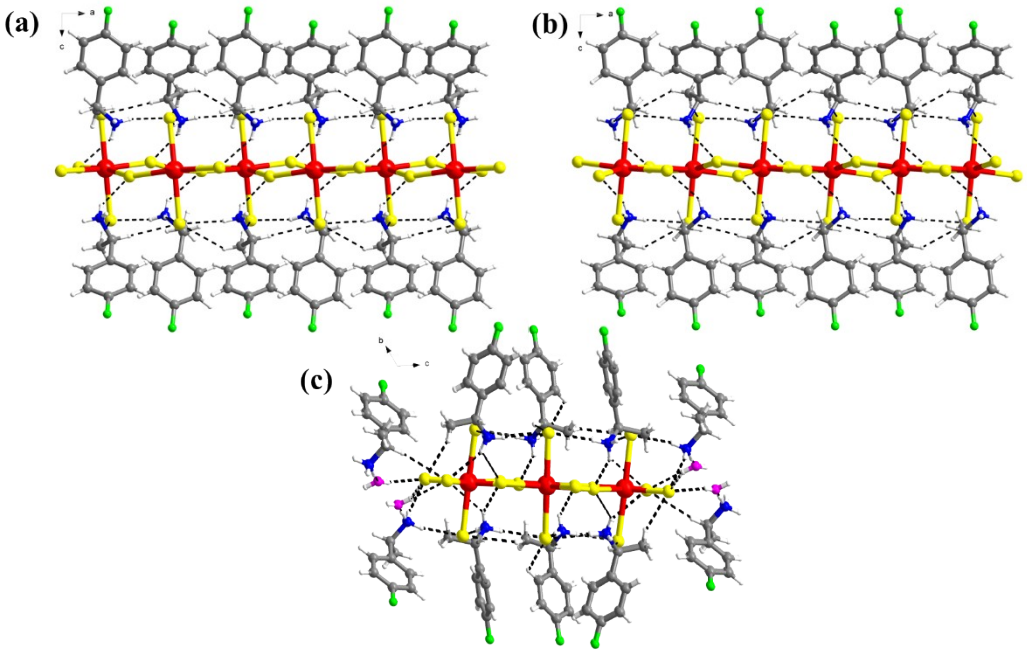

Fig. S1. Hydrogen bonding interactions of Br atoms with **FMBA**$^{+}$ spacer cations in (a) ***R*-1**, (b) ***S*-1** and (c) ***rac*-1**.

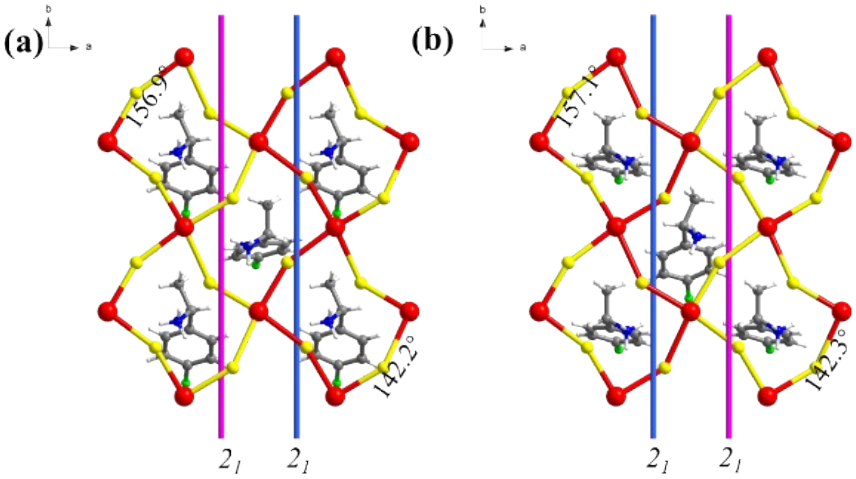

Fig. S2 (a) The plane view of [$PbBr_6$] the layers in (a) ***R*-1** and (b) ***S*-1** show two different equatorial Pb–Br–Pb bond angles, and the 2_1- axis that exists in the helical arrangement of different Br atoms on the equatorial plane (pink and blue).

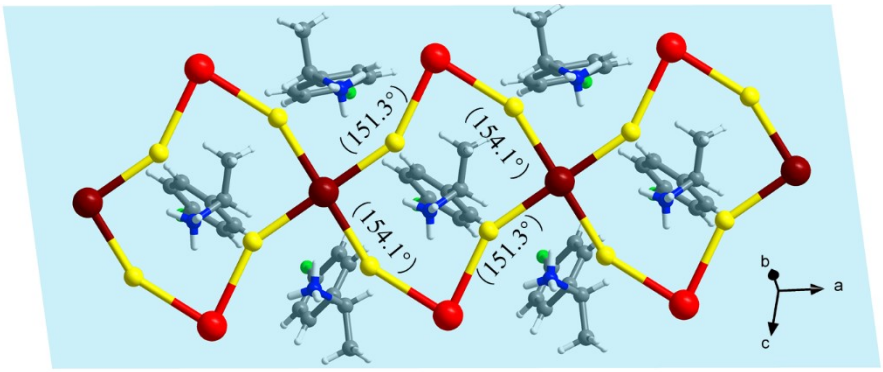

Fig. S3. Schematic diagram of the inorganic layer part of ***rac*-1**.

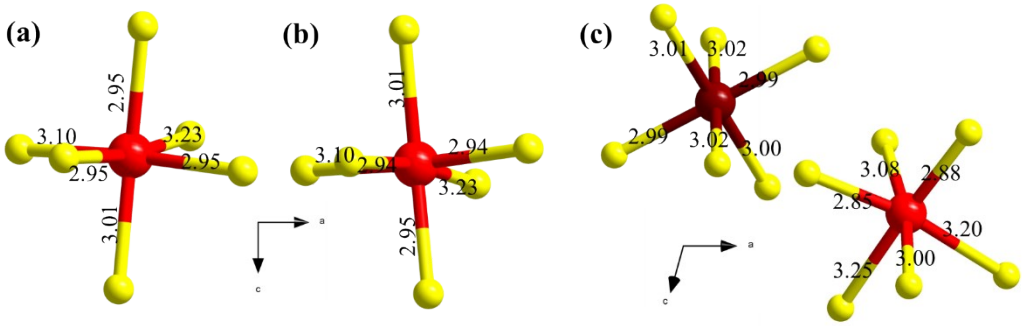

Fig. S4 $[PbBr_6]^{4-}$ octahedron in (a) ***R*-1**, (b) ***S*-1,** (b) ***rac*-1** (dark red: Pb1; red: Pb2).

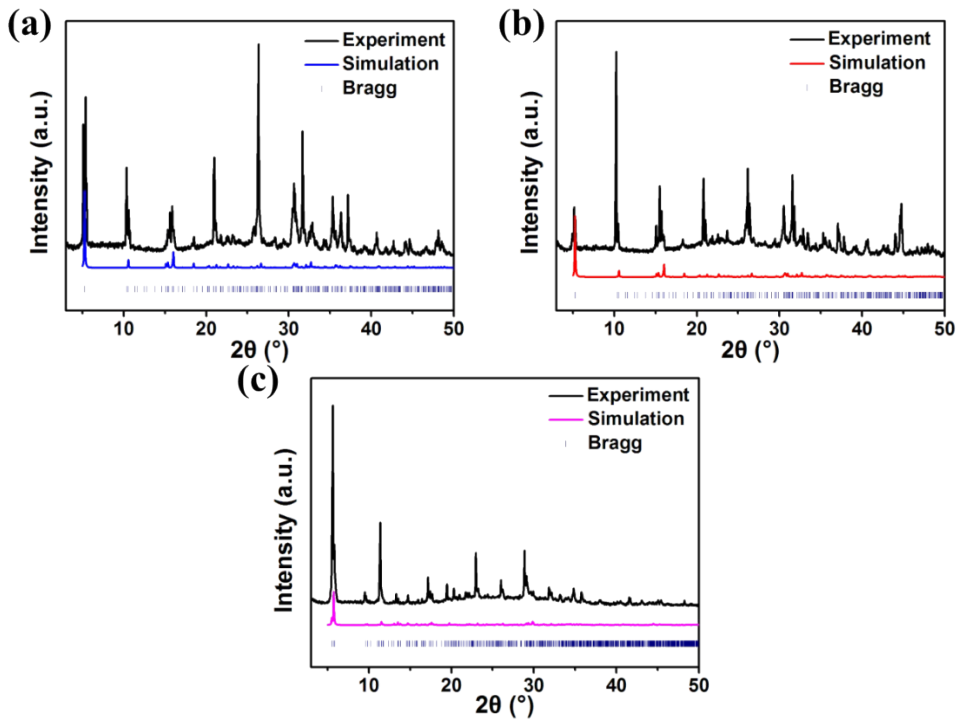

Fig. S5. PXRD patterns of our as-synthesized (a) ***R*-1**, (b) ***S*-1**, and (c) ***rac*-1**.

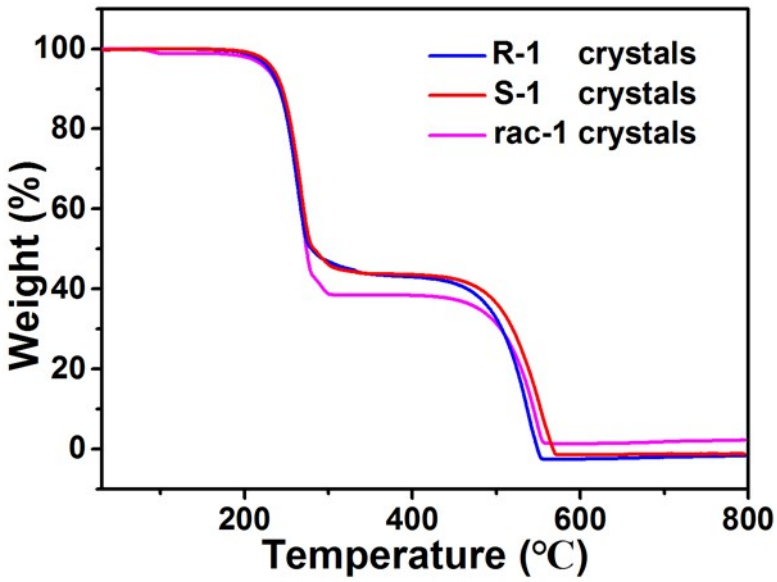

Fig. S6. TGA curve of ***R*-1**, ***S*-1** and ***rac*-1** crystals.

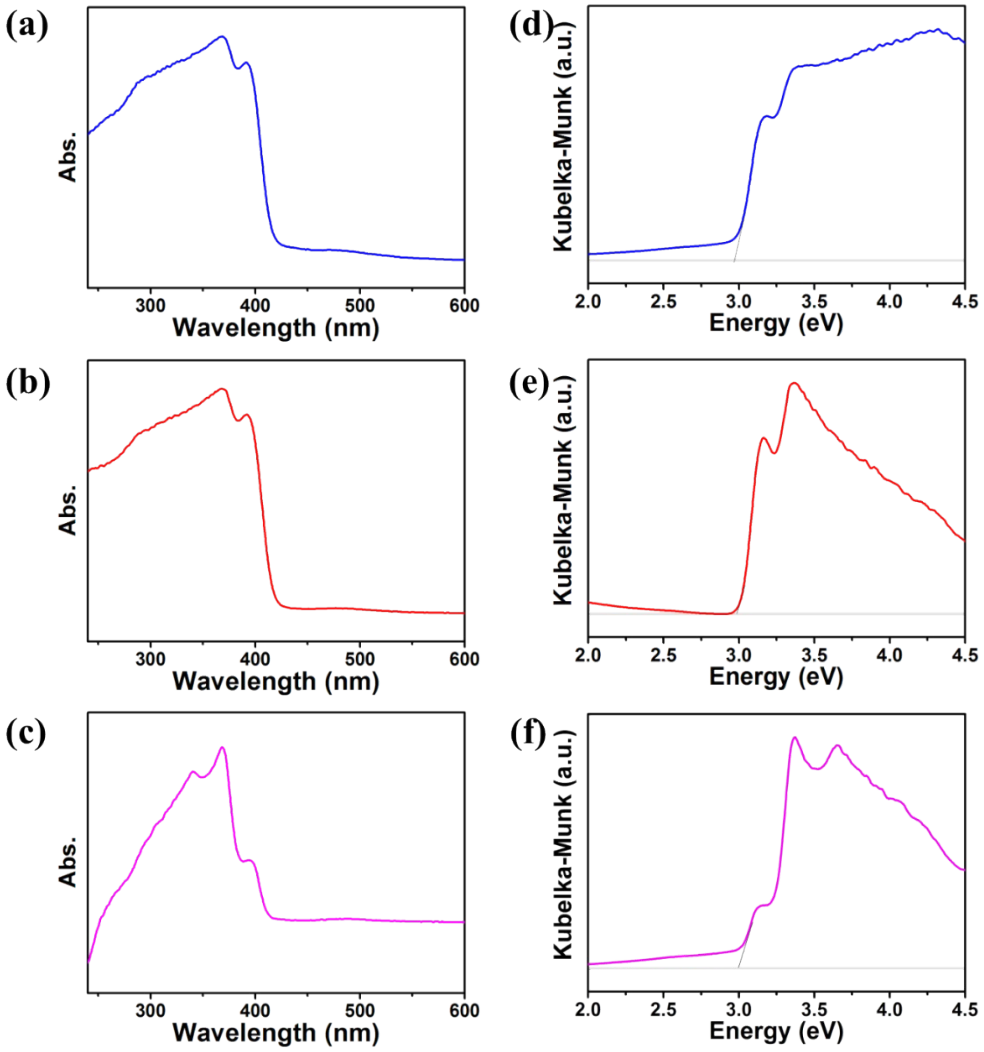

Fig. S7. The solid UV-vis spectra of (a) ***R*-1** (b) ***S*-1**, and (c) ***rac*-1.** The optical band gap diagrams of (d) ***R*-1**, (e) ***S*-1** and (f) ***rac*-1** are simulated according to the solid UV-Vis absorption and the Tacu equation.

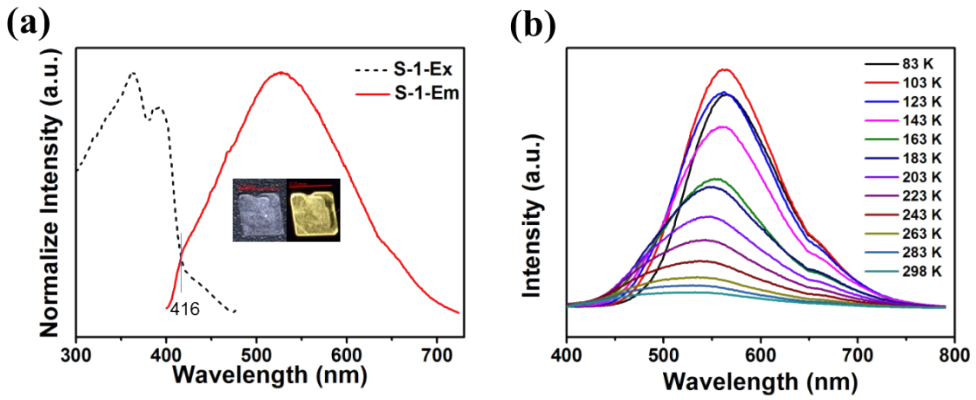

Fig. S8. (a) Excitation and luminescence profiles of ***S*-1**. Inset is a ***S*-1** fluorescent photograph. (b) Temperature-dependent PL spectra of ***S*-1**.

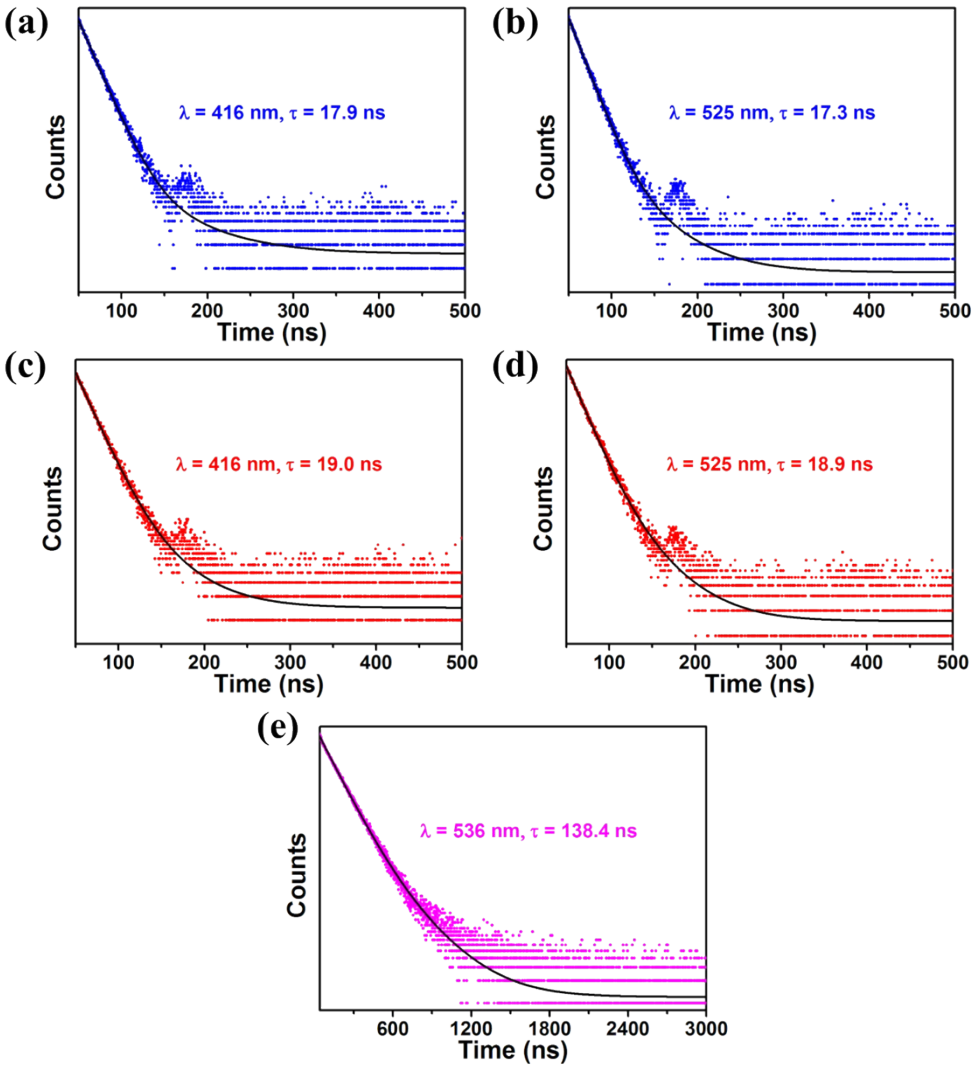

Fig. S9. Decay curves of (a, b) ***R*-1**, (c, d) ***S*-1** and (e) ***rac*-1** at 298 K.

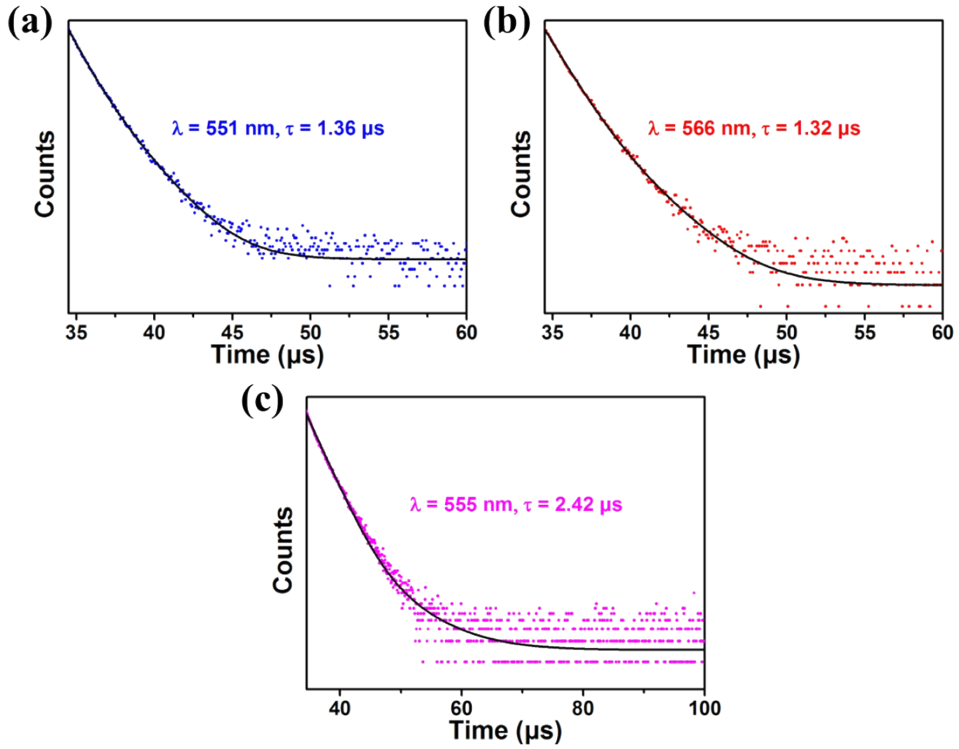

Fig. S10. Photoluminescent decay curves of (a) ***R*-1**, (b) ***S*-1** and (c) ***rac*-1** at 83 K.

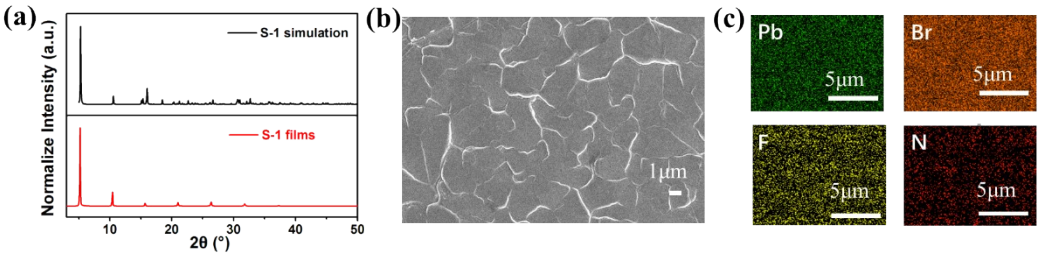

Fig. S11. (a) XRD pattern of ***S*-1** thin film and simulation pattern of corresponding single crystals. (b) SEM photograph of ***S*-1** films. (c) Mapping diagram of partial element distribution in specific places of ***S*-1** films.

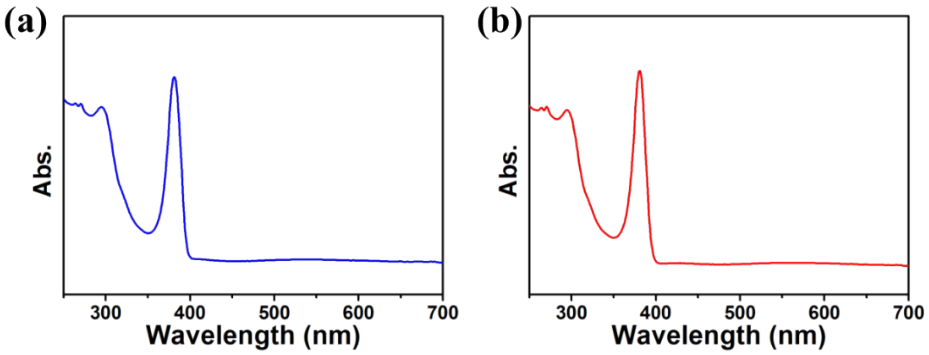

Fig. S12. UV-Vis absorption of (a) ***R*-1**, (b) ***S*-1** films.

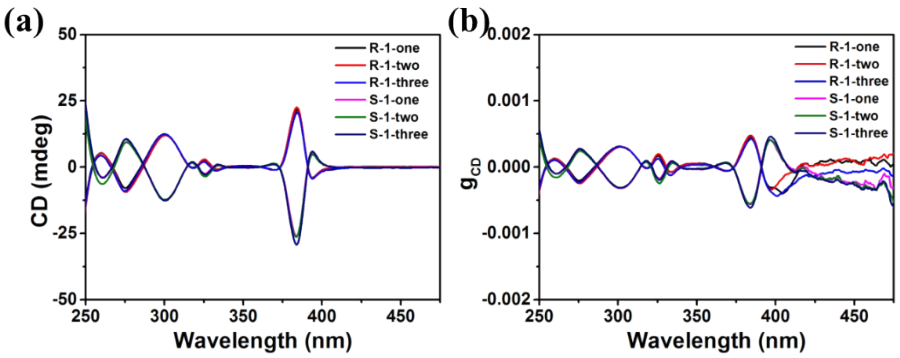

Fig. S13. (a) CD signals and (b) g_{CD} of ***R*-1** and ***S*-1** thin films with different sizes.

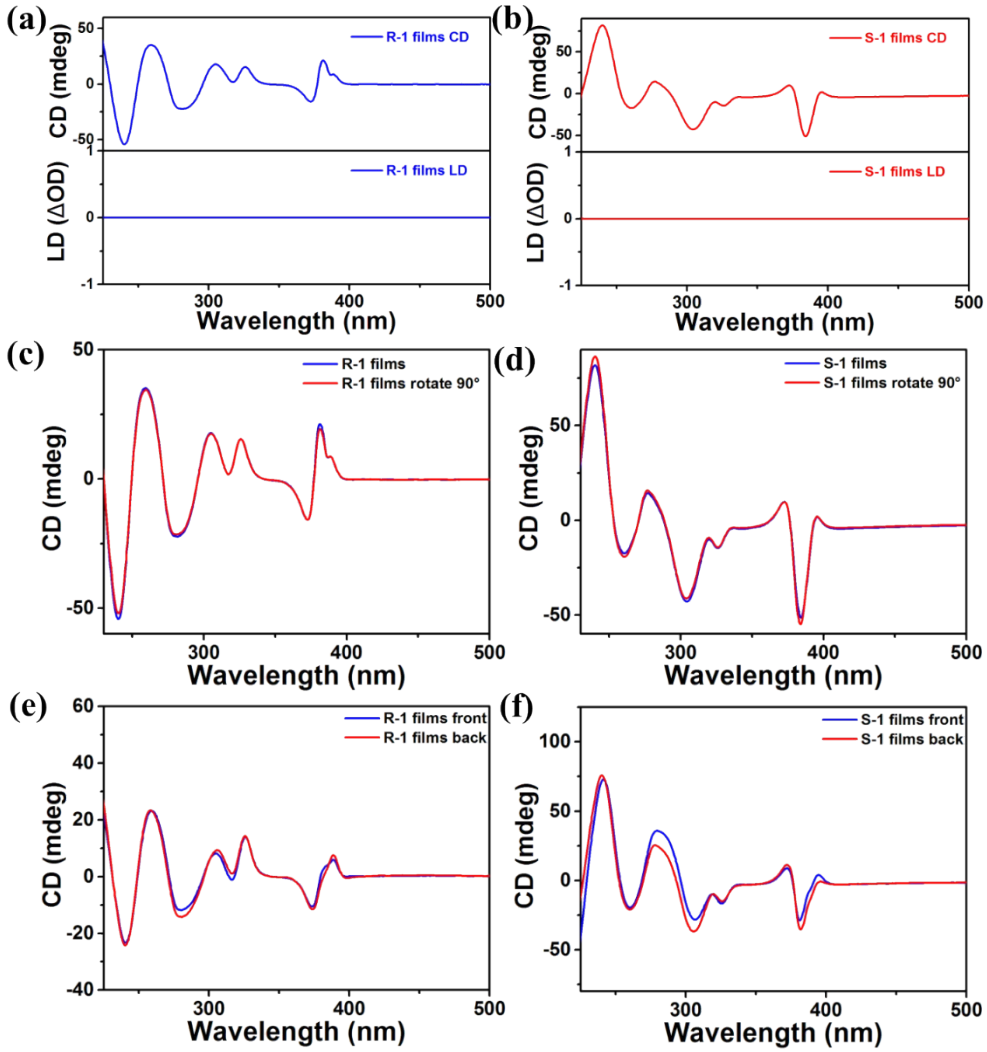

Fig. S14. (a, b) CD and LD spectra of ***R*/*S*-1** thin films. (c, d) CD signals from different azimuth (90°) of ***R*/*S*-1** thin films. (e, f) CD signals under flip of ***R*/*S*-1**thin films.

Supporting Tables

Table S1. Crystal data and structure refinement for *R*-1, *S*-1 and *rac*-1

Compound	***R*-1**	***S*-1**	***rac*-1**
Empirical formula	$C_{16}H_{22}Br_4F_2N_2Pb$	$C_{16}H_{22}Br_4F_2N_2Pb$	$C_{64}H_{92}Br_{14}F_8N_8O_2Pb_3$
Formula weight	807.18	807.18	2897.76
Temperature / K	200.00	200.00	296
Crystal system	orthorhombic	orthorhombic	triclinic
Space group	$P2_12_12_1$	$P2_12_12_1$	P-1
a /Å	7.84310(10)	7.84030(10)	8.1612(2)
b /Å	8.79770(10)	8.79580(10)	17.5034(4)
c /Å	33.4343(4)	33.4329(4)	18.6108(5)
α /°	90	90	115.7360(10)
β /°	90	90	102.2250(10)
γ /°	90	90	95.0980(10)
V /Å^3	2307.01(5)	2305.59(5)	2290.62(10)
Z	4	4	1
ρ_{calc} g/cm^3	2.324	2.325	2.101
μ /mm^{-1}	22.504	22.518	11.662
F(000)	1488.0	1488.0	1356.0
2Θ range for data collection /°	10.398 to 132.996	10.4 to 132.984	4.426 to 55.17
Reflections collected	7114	6740	133130
Data/restraints/parameters	3815/0/230	3744/0/231	7908/1/456
Goodness-of-fit on F^2	1.027	1.065	1.012
Final R indexes [I>=2σ (I)]	R_1 = 0.0310, wR_2 = 0.0726	R_1 = 0.0373, wR_2 = 0.1019	R_1 = 0.0281, wR_2 = 0.0565
Final R indexes [all data]	R_1 = 0.0344, wR_2 = 0.0741	R_1 = 0.0380, wR_2 = 0.1025	R_1 = 0.0468, wR_2 = 0.0616
Flack parameter	-0.028(8)	-0.013(10)	-
CCDC	2252841	2252843	2253014

***R*-1**: [1]2-X, -1/2+Y, 3/2-Z; [2]1-X, -1/2+Y, 3/2-Z; [3]2-X, 1/2+Y, 3/2-Z; [4]1-X, 1/2+Y, 3/2-Z

***S*-1**: [1]-X, 1/2+Y, 1/2-Z; [2]1-X,1/2+Y,1/2-Z; [3]-X, -1/2+Y,1/2-Z; [4]1-X, -1/2+Y,1/2-Z

***rac*-1**: [1]2-X, -1-Y,1-Z; [2]-1+X, +Y, +Z

Table S2. The main bond length in *R*-1, *S*-1, and *rac*-1.

***R*-1**		***S*-1**	
Bond	**(Å)**	Bond	**(Å)**
Pb1-Br1	3.0158(11)	Pb1-Br1	2.9483(11)
Pb1-Br2	2.9502(11)	Pb1-Br1[1]	3.2329(12)
Pb1-Br2[1]	3.2333(10)	Pb1-Br2	2.9530(11)
Pb1-Br3	2.9516(11)	Pb1-Br3	3.0170(11)
Pb1-Br4	2.9497(10)	Pb1-Br4[2]	3.1080(11)
Pb1-Br4[2]	3.1077(10)	Pb1-Br4	2.9462(11)
***rac*-1**			
Bond	**(Å)**	Bond	**(Å)**
Pb1-Br1[1]	3.0164(4)	Pb2-Br2[2]	3.2508(5)
Pb1-Br1	3.0164(4)	Pb2-Br3	3.2005(5)
Pb1-Br2[1]	2.9934(4)	Pb2-Br4	3.0792(5)
Pb1-Br2	2.9934(4)	Pb2-Br5	2.8792(5)
Pb1-Br3	3.0117(4)	Pb2-Br6	2.8455(5)
Pb1-Br3[1]	3.0117(4)	Pb2-Br7	3.0061(5)

Table S3. The major bond angles in *R*-1, *S*-1, and *rac*-1.

***R*-1**		***S*-1**	
Angle	(˚)	Angle	(˚)
Br1-Pb1-Br2^{1}	103.03(3)	Br1-Pb1-Br1^{1}	96.711(16)
Br1-Pb1-Br4^{2}	90.58(3)	Br1-Pb1-Br2	87.28(3)
Br2-Pb1-Br1	85.77(3)	Br1-Pb1-Br3	85.80(3)
Br2-Pb1-Br2^{1}	96.713(14)	Br1-Pb1-Br4^{2}	172.40(3)
Br2-Pb1-Br3	87.27(3)	Br2-Pb1-Br1^{1}	88.84(3)
Br2-Pb1-Br4^{2}	172.43(3)	Br2-Pb1-Br3	166.85(4)
Br3-Pb1-Br1	166.85(3)	Br2-Pb1-Br4^{2}	97.52(3)
Br3-Pb1-Br2^{1}	88.85(3)	Br3-Pb1-Br1^{1}	103.06(3)
Br3-Pb1-Br4^{2}	97.56(3)	Br3-Pb1-Br4^{2}	90.59(3)
Br4-Pb1-Br1	83.40(3)	Br4-Pb1-Br1^{1}	171.08(3)
Br4-Pb1-Br2^{1}	171.08(3)	Br4-Pb1-Br1	89.91(3)
Br4^{2}-Pb1-Br2^{1}	77.64(3)	Br4^{2}-Pb1-Br1^{1}	77.58(3)
Br4-Pb1-Br2	89.87(3)	Br4-Pb1-Br2	85.51(3)
Br4-Pb1-Br3	85.45(3)	Br4-Pb1-Br3	83.31(3)
Br4-Pb1-Br4^{2}	96.293(11)	Br4-Pb1-Br4^{2}	96.313(12)
***rac*-1**			
Angle	(˚)	Angle	(˚)
Br2^{1}-Pb1-Br1	91.982(13)	Br4-Pb2-Br3	99.196(13)
Br2-Pb1-Br1^{1}	88.020(13)	Br4-Pb2-Br5	90.911(15)
Br2-Pb1-Br1	88.017(13)	Br5-Pb2-Br2^{2}	177.472(15)
Br2^{1}-Pb1-Br1^{1}	91.981(13)	Br5-Pb2-Br3	94.202(14)
Br2-Pb1-Br3^{1}	93.525(13)	Br5-Pb2-Br4	90.911(15)
Br2-Pb1-Br3	86.475(13)	Br5-Pb2-Br7	94.954(15)
Br2^{1}-Pb1-Br3	93.524(13)	Br6-Pb2-Br2^{2}	86.808(14)
Br2^{1}-Pb1-Br3^{1}	86.476(13)	Br6-Pb2-Br3	169.941(13)
Br3-Pb1-Br1^{1}	86.265(12)	Br6-Pb2-Br4	83.565(14)
Br3^{1}-Pb1-Br1^{1}	93.734(13)	Br6-Pb2-Br5	95.428(15)
Br3^{1}-Pb1-Br1	86.268(12)	Br6-Pb2-Br7	88.780(14)
Br3-Pb1-Br1	93.733(12)	Br7-Pb2-Br2^{2}	83.898(13)
Br3-Pb2-Br2^{2}	83.507(12)	Br7-Pb2-Br3	87.498(13)
Br4-Pb2-Br2^{2}	90.512(14)	Br7-Pb2-Br4	170.769(15)

Table S4. Experimental hydrogen bonding parameters single crystal X-ray structures for HOIPs are studied in this work. The subscripts 'eq' and 'ax' indicate equatorial and axial directions respectively.

Compound	H-bond	length (Å)	angle at H (°)
***R*-1**	N-H---Br_{eq}	2.683	150.22
	N-H---Br_{eq}	2.694	128.47
	N-H---Br_{ax}	2.651	153.74
	N-H---Br_{ax}	2.647	162.62
	N-H---Br_{ax}	2.484	162.62
	N-H---Br_{ax}	2.543	165.18
	C-H---Br_{ax}	2.981	143.79
	C-H---Br_{ax}	3.084	139.91
	C-H---Br_{ax}	2.906	171.26
***S*-1**	N-H---Br_{eq}	2.706	128.20
	N-H---Br_{eq}	2.653	157.76
	N-H---Br_{ax}	2.526	165.54
	N-H---Br_{ax}	2.502	161.43
	N-H---Br_{ax}	2.596	164.07
	N-H---Br_{ax}	2.603	160.89
	C-H---Br_{ax}	3.116	138.93
	C-H---Br_{ax}	2.981	140.93
	C-H---Br_{ax}	2.902	173.25
***rac*-1**	N-H---Br_{eq}	2.735	135.58
	N-H---Br_{eq}	2.767	132.31
	N-H---Br_{eq}	2.913	146.88
	N-H---Br_{eq}	2.726	136.60
	N-H---Br_{eq}	3.025	127.61
	N-H---Br_{eq}	2.855	128.82
	N-H---Br_{ax}	2.474	163.23
	N-H---Br_{ax}	2.592	170.42
	N-H---Br_{ax}	2.709	165.97
	N-H---Br_{ax}	2.524	167.96
	N-H---Br_{ax}	2.620	166.72
	N-H---Br_{ax}	2.575	172.39
	N-H---Br_{ax}	2.524	165.92
	C-H---Br_{ax}	3.113	136.90
	C-H---Br_{ax}	3.098	123.58
	C-H---Br_{ax}	3.080	146.50
	O-H---Br_{eq}	2.702	156.08
	O-H---Br_{eq}	2.523	153.29

Supplementary References

1. CrysAlisPro, Version 1.171.36.31. Agilent Technologies Inc., Santa Clara, CA, USA 2012.

2. G. M. Sheldrick, Acta Cryst. A, 2008, 64, 112−122.

3. O. V. Dolomanov, L. J. Bourhis, R. J. Gildea, J. A. K. Howard and H. Puschmann, J. Appl. Cryst., 2009, 42, 339−341.

4. G. M. Sheldrick, Acta Cryst. C, 2015, 71, 3−8.